Accepted Manuscript

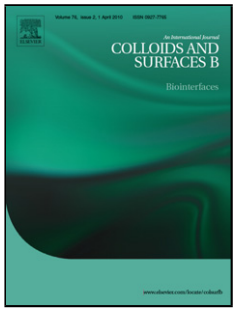

Title: Microfluidic synthesis of multifunctional liposomes for tumour targeting

Author: Rui Ran Anton P.J. Middelberg Chun-Xia Zhao

PII: S0927-7765(16)30670-1
DOI: http://dx.doi.org/doi:10.1016/j.colsurfb.2016.09.016
Reference: COLSUB 8148

To appear in: *Colloids and Surfaces B: Biointerfaces*

Received date: 20-7-2016
Revised date: 9-9-2016
Accepted date: 11-9-2016

Please cite this article as: Rui Ran, Anton P.J.Middelberg, Chun-Xia Zhao, Microfluidic synthesis of multifunctional liposomes for tumour targeting, Colloids and Surfaces B: Biointerfaces http://dx.doi.org/10.1016/j.colsurfb.2016.09.016

Microfluidic synthesis of multifunctional liposomes for tumour targeting

*Rui Ran, Anton P.J. Middelberg, Chun-Xia Zhao**

Australian Institute for Bioengineering and Nanotechnology, The University of Queensland, St. Lucia QLD 4072, Australia

* Corresponding author

E-mail: z.chunxia@uq.edu.au

Address: Australian Institute for Bioengineering and Nanotechnology, The University of Queensland, St. Lucia QLD 4072, Australia

Graphical abstract

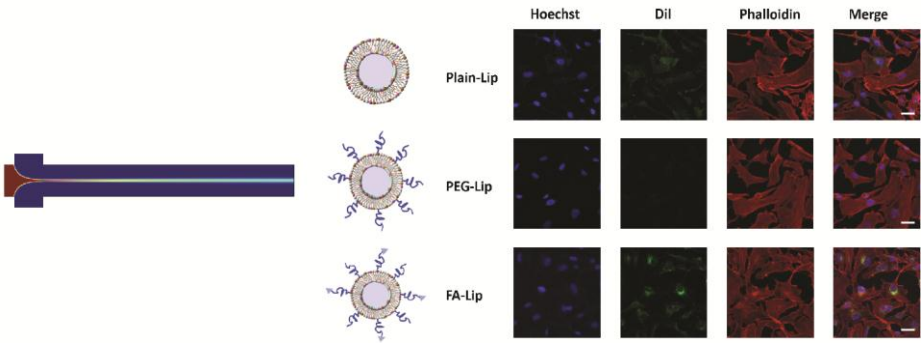

Highlights

- Targeted liposomes can be prepared in the one-step microfluidic device
- Size and surface properties can be controlled easily
- This microfluidic method directed targeted liposomes possess selective cell uptake enhancement in both 2D and 3D model.
- At the same time, these liposomes can reduce phagocytosis.

Abstract

Nanotechnology has started a new era in engineering multifunctional nanoparticles for diagnosis and therapeutics by incorporating therapeutic drugs, targeting ligands, stimuli-responsive release and imaging molecules. However, more functionality requires more complex synthesis processes, resulting in poor reproducibility, low yield and high production cost, hence difficulties in clinical translation. Herein we report a one-step microfluidic method for making multifunctional liposomes. Three formulations were prepared using this simple method, including plain liposomes, PEGylated liposomes and folic acid functionalised liposomes, all with a fluorescence dye encapsulated for imaging. The size and surface properties of these liposomes can be precisely controlled by simply tuning the flow rate ratio and the ratio of the lipids to PEGylated lipid (DSPE-PEG_{2000}) and to the DSPE-PEG_{2000}-Folate, respectively. The synthesised liposomes remained stable under mimic serum conditions. Compared to the plain liposomes and PEGylated liposomes, the targeted folic acid functionalised liposomes exhibited enhanced cellular uptake by the FA receptor positive SKOV3 cells, but not the negative MCF7 cells, and this enhanced uptake could be inhibited by adding excess free folic acid, indicating high specificity of FA ligand-receptor endocytosis. Further evaluation using the 3D tumour spheroid model also showed higher internalisation of the targeted liposome formulation in comparison with the PEGylated one. To the best of our knowledge, this work demonstrates for the first time the versatility of this microfluidic method for making different liposome formulations in a single step, their superior physicochemical properties as well as the enhanced cellular uptake and tumour spheroid uptake of the targeted liposomes.

Keywords: Microfluidic, targeted liposome, controllability, biological activity

1. Introduction

Liposomes are artificially constructed nanostructures inspired by the composition and structure of cell membranes. Liposomes have been studied extensively in the past decades because of their superior properties over other nanosystems, such as non-toxicity, non-immunogenicity, and good biocompatibility and biodegradability. By 2014, fifteen lipid-based therapeutics have gained clinical approval, such as Doxil [1], DaunoXome, etc., for the treatment of cancer, fungi, microbes, analgesia, etc., and more are undergoing clinical trials [2].

Different methods have been developed for producing liposomes, such as thin-film hydration, freeze-drying, detergent depletion and alcohol injection [3]. These conventional methods are all based on bulk synthesis, and require post-processing steps (extrusion or sonication) to homogenise the size. Multifunctional liposomes need more post-processing steps, such as post-conjugation steps to add a targeting ligand and/or to conjugate imaging molecules, resulting in big batch-to-batch variations and poor control over their size and surface properties, which play key roles in determining their behaviour *in vivo* [4]. The difficulties in manufacturing multifunctional liposomes for targeted delivery limits their large-scale production, which is one of the reasons that no active targeted liposome has gained clinical approval, even though significant amount of work has been directed to make multifunctional liposomes. Therefore, it is of great significance to develop a robust platform technology for preparing multifunctional liposomes with reproducible and precisely controlled properties.

Microfluidic technology has emerged as an alternative to bulk methods for synthesising various materials in recent years [5-7]. The microfluidic hydrodynamic flow focusing (HFF) method has demonstrated its versatility in making various kinds of nanomaterials through self-assembly, including polymeric nanoparticles [8], liposomes [9] and lipid-polymer hybrid nanoparticles [10]. This HFF method allows the formation of liposomes through a single-step self-assembly. Basically, a lipid-containing alcohol solution that is introduced from the central microchannel mixes with an aqueous buffer solution from the vertical channels. As the alcohol diffuses to the aqueous buffer, the lipid materials solubilised in the alcohol becomes less soluble and self-assembles into planar lipid bilayer discs. Subsequently, these lipid discs bend to reduce the exposure of the hydrophobic lipid chain to the hydrophilic buffer and finally close into spherical liposomes [11]. This single-step method offers better control over the properties of liposomes, such as particle size, size distribution and surface properties (PEGylation and targeting ligand) [11-14]. More importantly, this method can be easily scaled up. Hood et al.

recently reported the high throughput production of liposomes using a high aspect ratio HFF device. The production rate was as high as 95 mg h^{-1}, which was approximately 1000 times higher than using the original HFF device [15]. Furthermore, the production throughput can be increased through parallelization [16]. Therefore, microfluidic technology holds great potential in producing liposomes for practical applications. However, current work has been focusing on designing various microfluidic devices for making liposomes, while little effort has been made to synthesise multifunctional liposomes (PEGylated and targeted liposomes). To the best of our knowledge, none have investigated their biological functions, which are critical to assess whether the liposomes prepared in microfluidic devices have the correct conformation and thus biological function.

In this study, three liposome formulations, that is, plain liposomes, PEGylated liposomes, and an active targeting ligand – folic acid modified liposomes, were prepared using the single-step microfluidic hydrodynamic flow focusing method. Size, polydispersity and surface properties of the three liposome formulations as a function of flow rate ratios were investigated. Their biological functions were systemically studied *in vitro* using both the two-dimensional cell monolayer model and the three-dimensional tumour spheroid model. Other properties such as serum stability and phagocytosis were also investigated.

2. Materials and methods

2.1 Materials

1,2-dimyristoyl-sn-glycero-3-phosphocholine (DMPC), 1,2-distearoyl-sn-glycero-3-phosphoethanolamine-N-[methoxy(polyethylene glycol)-2000] (ammonium salt) (DSPE-PEG_{2000}) were purchased from Avanti Polar Lipids (Alabaster, AL, USA). Cholesterol, dihexadecyl phosphate (DCP), histology mounting medium, paraformaldehyde, Accumax solution were obtained from Sigma-Aldrich (St. Louis, MO, USA). Mouse anti-human folate binding protein antibody was purchased from Abcam (Cambridge, UK). Alexa Fluor® 488 conjugate goat anti-mouse IgG secondary antibody, Hoechst 33342 and Alexa Fluor® 647 Phalloidin were purchased from Invitrogen (Carlsbad, CA, USA). 1,2-distearoyl-sn-glycero-3-phosphoethanolamine-N-[folate(polyethylene glycol)-2000] (DSPE-PEG_{2000}-Folate) was obtained from Nanocs (NYC, NY, USA). Other chemicals and reagents were of analytical grade.

2.2 Microfluidic device fabrication

The microfluidic device was fabricated using photolithography and soft lithography. The microchannel pattern was designed using the AutoCAD software and was printed to a chrome mask. For SU-8 master fabrication (photolithography), SU-8 was spin-coated to a clean 4-inch silicon wafer, followed by ultraviolet exposure using the patterned chrome mask as the template. After baking, developing and washing, the SU-8 master was ready to use. Soft lithography was conducted by pouring Polydimethylsiloxane (PDMS) over the SU-8 master mold, followed by incubation at 80 °C for 30 min. The cross-linked PDMS was peeled off from the SU-8 master mold, and then holes were punched at inlets and outlets. Finally, the PDMS layer was bonded to a glass slide coated with a thin layer of PDMS to form a microfluidic device.

2.3 Preparation and characterisation of liposomes

For making Plain-Lip (liposomes without surface modification), DMPC, cholesterol and DCP were dissolved in chloroform at a molar ratio of 55:40:5. For PEG-Lip, DMPC, cholesterol, DCP and DSPE-PEG_{2000} were dissolved in chloroform at a molar ratio of 47:40:5:8; while for FA-Lip, the molar ratio of DMPC, cholesterol, DCP, DSPE-PEG_{2000} and DSPE-PEG_{2000}-Folate was 47:40:5:4:4. After mixing, chloroform was removed using a rotary evaporator and the dried lipid film was then dissolved in anhydrous isopropanol using a total lipid concentration of 10 mM. For DiI labelled liposome, the dried lipid film was dissolved in anhydrous isopropanol containing 10 µg/mL DiI. The lipid containing isopropanol solution was then passed through a 0.22 µm filter and degassed before introduced to the microfluidic device.

Liposomes were formed by injecting the lipid containing isopropanol solution to the central stream in the microfluidic chip and squeezed by the phosphate buffer solution (PBS) stream from the two vertical channels. The flow rate ratio (FRR) which represents the volumetric flow rate of PBS to isopropanol varied from 4:1, 8:1, 12:1 to 16:1. The total flow velocity of the fluid stream in the liposome mixing channel was kept at 0.4 m/s, corresponding to a total volumetric flow rate of 28.8 µL/min. The synthesis of liposomes in this hydrodynamic flow focusing device procedure was monitored using an inverted optical microscope (Nikon, Tokyo, Japan). The size, polydispersity index (PDI) and zeta-potential of the liposomes synthesised were determined using a Zetasizer Nano ZS (Malvern Instruments, Worcestershire, UK). The morphology of Plain-Lip, PEG-Lip and FA-Lip at FRR=12:1 were observed using a transmission electron microscopy (Jeol, Tokyo, Japan). Samples were dropped onto a copper

TEM grid with a carbon film and air-dried at room temperature followed by negative-staining using 1% uranyl acetate.

2.4 *In vitro* stability of liposomes in fetal bovine serum (FBS)

In order to investigate the stability of liposomes in the presence of a mimic serum environment, liposomes were incubated with an equal volume of FBS under 37 ˚C with gentle shaking at 30 rpm. At different time points (1 h, 2 h, 4 h, 8 h, 12 h and 24 h), samples were collected and diluted for the size measurement by a Zetasizer Nano ZS instrument. The same incubation process was also conducted in 96 well plate and the absorbance at 680 nm (A) was measured at different time point and recorded using a microplate reader. The relative turbidity at 0 h was set to be 1 and at other time points was calculated as $A_{sample}/A_{0\,h}$.

2.5 Cell lines and cell culture

RAW264.7 cells (murine macrophage cells), SKOV3 cells (human ovarian adenocarcinoma cells) and MCF-7 cells (human breast adenocarcinoma cells) were purchased from American Type Culture Collection (ATCC), and were cultured in high glucose DMEM medium supplemented with 10% FBS, 100 U/mL penicillin and 100 U/mL streptomycin at 37 ˚C in a humidified 5% CO_2 atmosphere.

2.6 Macrophage cell uptake

RAW 264.7 cells were seeded into a 24 well plate at a density of 2.5×10^5 cells/well one day prior to the experiment. The next day, DiI labelled Plain-Lip, PEG-Lip and FA-Lip were added into each well at a final lipid concentration of 38 μM. Cells cultured with liposome-free medium was regarded as the blank group. After 4 h incubation under 37 ˚C, cells were collected, washed three times with PBS, and then resuspended in 0.5 mL PBS. The fluorescent intensity was measured using a flow cytometer with the excitation wavelength at 549 nm and the emission wavelength at 565 nm. Ten thousand cells were recorded and analysed for each sample.

2.7 Determination of folate receptor expression

The folate receptor expression of SKOV3 and MCF-7 cells was determined using a primary antibody and a fluorescence conjugated secondary antibody. Briefly, SKOV3 cells or MCF-7 cells were seeded into 24 well plate at a density of 2.5×10^5 cells/well. After the cells have reached a proper density, they were collected, washed with PBS and resuspended to 1×10^6

cells/mL in ice cold PBS containing 1% BSA and 0.5% sodium azide (buffer solution), then incubated the cells with the mouse anti-human folate binding protein primary antibody at a concentration of 10 µg/mL in an ice cold buffer solution. After 30 min, cells were washed three times and resuspended in a buffer solution containing 10 µg/mL Alexa Fluor® 488 conjugate goat anti-mouse IgG secondary antibody. After incubation for 30 min, cells were again washed three times and resuspended in 0.5 mL buffer solution for flow cytometry analysis. The excitation and emission wavelengths were set at 496 nm and 519 nm, respectively. Ten thousand cells were collected for each sample. Cells incubated with the secondary antibody were regarded as the control group while cells incubated with both primary and secondary antibodies were considered as the sample group.

2.8 Tumour monolayer cellular uptake study

2.8.1 Qualitative observation using Confocal Laser Scanning Microscopy (CLSM)

SKOV3 or MCF-7 cells at a density of 1×10^5 cells/well were seeded into a 24-well flat bottom tissue culture plate with a diameter of 12 mm glass slips and incubated at 37 °C with 5 % (v/v) CO_2 supplied. After 24 h, DiI labelled liposomes were added to each well at a final lipid concentration of 38 µM and allowed for further incubation for 4 h. Then the cells were washed with PBS for three times, followed by fixation with 4% paraformaldehyde at room temperature for 10 min. Prior to staining the cytoskeleton, fixed cells were treated with 0.1% Triton X-100 for 5 min and 1% BSA containing PBS solution for 30 min. After that, cells were incubated with Alexa Fluor® 647 Phalloidin for 30 min, followed by the nucleus staining using Hoechst 33342. Finally, coverslips were mounted to glass slides using histology mounting medium and observed using a CLSM (Zeiss 710, Jena, Germany).

2.8.2 Quantitative flow cytometry measurement

SKOV3 and MCF-7 cells were seeded into a 24 well plate at a density of 2.5×10^5 cells/well and allowed for attachment for 24 h. The next day, DiI labelled Plain-Lip, PEG-Lip and FA-Lip were added to the corresponding wells to a final lipid concentration of 38 µM and incubated under 37 ˚C. For competitive inhibition experiments, prior to adding the liposomes, free folic acid was added to the medium at a final concentration of 1.5 mM (about 1000 times of the folate concentration in the FA-Lip). Cells cultured with liposome-free medium were regarded as the blank group. After incubation for 4 h, cells were trypsinised, collected, washed with PBS for three times and then resuspended in 0.5 mL PBS. Fluorescent intensity was measured with

the excitation and emission wavelengths at 549 nm and 565 nm, respectively, using a flow cytometer.

2.9 3D tumour spheroid uptake

To establish the tumour spheroid model, SKOV3 or MCF-7 cells at a density of 5×10^3 cells/well were seeded into a 96 well plate which was pre-coated with 50 µL 2% low melting point agarose, then applied with centrifugation (1000g, 10 min) to initiate the formation of spheroids. They were monitored with an optical microscope and were ready to use after 7 days. Then DiI labelled liposomes were incubated with spheroids for 24 h and followed by washing with PBS and fixation with 4% paraformaldehyde. At last, spheroids were subjected to a confocal microscope. For the quantitative analysis, after incubation with DiI labelled liposomes for 4 h, 10 spheroids for each group were gathered and treated with 200 µL Accumax solution for 30 min at 37 °C with pipetting every 10 min. After dissociation, cells were washed three times with PBS and then analysed using a flow cytometry.

2.10 Statistical analysis

Statistical analysis were performed by the one-way ANOVA for multiple groups, and *p* value <0.05, <0.01 and <0.001 was marked as *, ** and ***, respectively.

3. Results and discussion

3.1 Microfluidic synthesis of three liposome formulations

Figs. 1A and 1B show the numerical simulation result and the photograph of liposome synthesis in the microfluidic hydrodynamic flow focusing (HFF) device under a microscope. The widths of the central channel and the two vertical channels are 20 µm, the height of the device is 60 µm and the total length of the central channel is 1 cm. To synthesise liposomes, the IPA stream containing the lipids was injected to the central channel and was intersected by the PBS buffer from the two side channels. During this process, the lipids solubilised in the IPA gradually self-assembled into liposomes due to their decreased solubility. By dissolving different lipids into the IPA phase, liposomes with different formulations could be formed in the same microfluidic device (Fig. 1C). The addition of an anionic surfactant DCP to the lipid solution was to prevent the aggregation of the non-PEGylated liposomes in the microfluidic device [14]. Three liposome formulations including plain liposome (Plain-Lip), PEGylated liposome (PEG-Lip) and folate targeted liposome (FA-Lip) were synthesised using this simple HFF device (Fig. 1C). The size and zeta potential of these liposomes can be easily controlled by adjusting the

flow rate ratio (FRR) of the volumetric flow rate of the PBS to that of the IPA phase. The density of PEG and the targeting ligand folate acid can be tuned by adjusting the components of the lipids solubilised in the IPA solution. For PEG-Lip, the PEG density was 8% while for FA-Lip, the FA density was 4% and the total PEG density was still kept at 8%.

3.2 Liposome size and surface properties

The size and surface properties of liposomes play important roles in determining their behaviour *in vivo*, including blood circulation time, accumulation in tumour site, vascular to tumour transfer and retention in tumour site. Normally, liposomes with a diameter of 90-200 nm show the longest blood half-lives [17], best tumour accumulation [17, 18] and tumour retention [19]. The size homogeneity can also affect the biodistribution of liposomes. Liposomes with a narrower size distribution showed a lower liver and spleen accumulation [20]. Neutralised liposomes and PEGylated liposomes also exhibited longer blood circulation time and better tumour accumulation [21]. Therefore, it is vital to prepare liposomes with uniform size and controlled surface properties.

The effects of the flow rate ratio of the IPA to the PBS phase (4:1, 8:1, 12:1 and 16:1) on particle size, particle size distribution index (PDI) and zeta-potential of the three formulations were systematically investigated. The size of the three liposomes all decreased with increasing the flow rate ratio. A non-equilibrium kinetic model can be used to explain the formation of the liposomes. This model proposes that two parameters, i.e., the growth time of the lipid discs and the rate of closing the discs into spherical vesicles, determine the liposome size [11]. Higher FRRs result in a thinner alcohol stream thus a thinner diffusion layer, so that the growth time of the lipid discs becomes shorter. Also, as the alcohol concentration decreases rapidly at higher FRRs, the discs closes faster [22]. Therefore, higher FRRs produce smaller liposomes. At a FRR of 12:1, the average sizes of Plain-Lip, PEG-Lip and FA-Lip were 108 ± 4 nm, 56 ± 1nm and 92 ± 3 nm, respectively. The PEGylated liposomes showed the smallest size compared to Plain-Lip and FA-lip, which is consistent with previous studies [23]. The addition of DSPE-PEG-FA led to a slight increase of the liposome size. Fig. 2B shows the PDI of the three liposomes indicating that this HFF method produced liposome particles with narrow size distribution with all PDIs below 0.2. For the Plain-Lip, the PDI decreased with the flow rate ratio, but for the other two formulations, no obvious trend was observed. At a FRR of 12:1, the PDI of plain, PEG and FA-Lip was 0.09 ± 0.01, 0.13 ± 0.01 and 0.14 ± 0.02, respectively.

As expected, the Plain-Lip exhibited a negative charge at approximately -10 mV due to the presence of negatively charged DCP, which was increased to about zero by simple PEGylation because of the charge screening effect of the PEG_{2000}. The FA-lip showed similar zeta potential as that of the PEG-Lip, indicating that the addition of DSPE-PEG_{2000}-Folate didn't change the surface charge. At a FRR of 12:1, the zeta-potential of Plain-Lip, PEG-Lip and FA-Lip was -9.5 ± 0.9 mV, -0.8 ± 0.4 mV and -0.9 ± 0.1 mV, respectively. The morphology of all the liposomes was observed using TEM, showing crumped and deformed shapes due to the vacuum conditions under TEM. The sizes of PEG-Lip and FA-Lip were smaller than that of the Plain-Lip (Fig. 2D), which is in consistence with the DLS measurement. The lipid bilayer structure could be observed clearly.

In this study, liposomes synthesised at the FRR of 12:1 were selected for the following *in vitro* experiments, including serum stability, macrophage uptake, two-dimensional cell monolayer and three-dimensional tumour spheroids uptake. To label the liposomes, DiI (10 µg/mL) was dissolved in the IPA solution along with the lipids. DiI labelled Plain-Lip, PEG-Lip and FA-Lip showed the same size, PDI and zeta potential as those unlabelled ones (data not shown).

of independent samples). (D) TEM images of Plain-Lip, PEG-Lip and FA-Lip. Scale bar represents 100 nm.

3.3. Serum stability

Liposome stability against physiological condition is a vital prerequisite for its *in vivo* use. To study their serum stability, liposomes were incubated with 50 % FBS to mimic the interactions with the serum *in vivo*. Two important parameters, turbidity and particle size, were monitored for 24 h. The relative turbidity for the three liposome formulations remained stable at approximately 1.0 (Fig. 3A). Additionally, the mean diameter of these liposomes didn't change much over the 24 h period of time (Fig. 3B). These results demonstrated the good stability of these three liposome formulations in physiological mimicking conditions. Two major factors contribute to the good stability of the three liposome formulations. Firstly, the surface property of nanoparticles plays key roles in determining their serum stability. As serum proteins are negatively charged, they are prone to interact with positively charged nanoparticles thus leading to aggregation through electrostatic interactions. So the negatively charged Plain-lip showed good stability because of the repulsion between the liposomes and serum proteins [24]. Secondly, PEGylation can also increase serum stability by excluding the serum protein binding and adhesion through steric repulsion. Therefore, even though the PEG-lip and FA-lip had very low surface charge, they were still able to remain stable in the serum [25].

3.4 Cellular uptake of liposomes by RAW 264.7 macrophage cells

Macrophage is a type of white blood cells involved in the innate immunity that recognises and destructs cell debris and foreign substances, such as pathogens and particles. It has been widely accepted that high macrophage uptake correlates with short circulation time. To achieve long circulation, the macrophage uptake needs to be minimised. PEGylation is a widely used method to evade the immune system and thus prolong the circulation time. Fig. 4 shows the RAW 264.7 cell uptake of the three liposome formulations. Compared to Plain-Lip, PEG-Lip and FA-Lip had significantly decreased cell uptake, which is consistent with previously reported results [26, 27]. This reduced phagocytosis of the PEG-Lip and FA-Lip is essential for a longer circulation time *in vivo*, which favours their accumulation in tumour sites. Furthermore, it has been noted that PEG-Lip and FA-Lip had different particle size (55 nm and 90 nm, respectively), but they possessed similar phagocytosis efficiency. It has been shown in some studies that particles with larger size have higher macrophage uptake [28]. However in our case the particle size didn't have any effect on the uptake probably because the sizes of PEG-Lip and FA-lip are both smaller enough to avoid phagocytosis.

3.5 Folate receptor expression

Folate receptor was first discovered as a tumour marker on a human ovarian carcinoma cell line in 1991 [29], and then approximately 90% of ovarian carcinomas as well as other cancer cells, including breast, kidney, lung brain, etc. were reported to overexpress the folate receptor [30]. The human ovarian carcinoma SKOV3 is a widely used folate receptor positive cell line, however for human breast carcinoma MCF-7 cell line, different literature reports quite contradictory folate receptor expression levels. Jie et al. employed MCF-7 as a folate receptor overexpressed cell line [31] while Haimei et al. used MCF-7 as a negative control [32]. In this study, we tested the folate receptor expression level of the MCF-7 and SKOV3 cell lines. Fig. 5 shows that MCF-7 cells have negligible folate receptor expression while SKOV3 cells possessed eighteen times higher expression. Therefore, SKOV3 cells were used as the folate receptor positive cells while MCF-7 cells were employed as the negative control.

3.6 Two-dimensional cellular uptake study

The ligand-receptor targeting efficiency of FA-Lip was explored using the two cell lines MCF-7 and SKOV3, as the folate receptor negative and positive cells, respectively. Fig. 6 shows qualitative (confocal microscopy) and quantitative (flow cytometry) results of cellular uptake of Plain-Lip, PEG-Lip and FA-Lip. Plain-Lip exhibited significant cellular uptake by both MCF-7 and SKOV3 cells after 4 h incubation, which was due to non-specific endocytosis [33]. In contrast, PEG-Lip showed negligible uptake by both the MCF-7 and SKOV3 cells as a result of the PEGylation, demonstrating its excellent capabilities in decreasing the non-specific cellular uptake by not only macrophage cells but also the non-phagocytic cells, which is called the "PEG dilemma" [34]. It was reported that the addition of 5 mol % of PEG to the surface of liposomes could drastically inhibit the binding and uptake of liposomes [35]. To enhance the specific cellular uptake while at the same time decreasing the non-specific phagocytosis by immune cells, PEGylation in combination with active targeting could be an option [36, 37]. Further incorporation of 4 mol % FA to PEG-Lip created an active targeting liposome (FA-Lip). The cellular uptake experiments confirmed that the addition of FA promoted enhanced uptake by the FA receptor positive SKOV3 cells, but not the receptor negative MCF-7.

Quantitative analysis by flow cytometry (Fig. 6C) illustrated a trend consistent with qualitative observations. Plain-Lip showed non-specific uptake by both MCF-7 and SKOV3 cells. FA-Lip and PEG-Lip had low and comparable uptake by MCF-7 cells, while the uptake of the FA-Lip by SKOV3 cells was 78% higher than that of the PEG-Lip. To demonstrate that the enhanced uptake by SKOV3 was receptor-mediated endocytosis, 1.5 mM of free folic acid was added along with the FA-Lip for the competitive uptake experiment, which was about 1000 times higher than the folate fraction of the FA-Lip. The addition of free folic acid considerably decreased the uptake of FA-Lip by SKOV3 cells, confirming ligand – receptor mediated endocytosis. It should be noted that the concentration of free folic acid was extremely high to ensure successful blocking of the cellular uptake, indicating the high specificity of the FA ligand-receptor endocytosis, possibly due to its multivalent interaction with the receptor [38, 39]. It has been reported in some studies that a molar fraction of as low as 0.03% DSPE-PEG-FA in a liposome formulation was sufficient for effective interaction with the folate receptor [40]. In this study, we found that when the total PEG density was 8%, FA density less than 4% was unable to achieve enhanced cellular uptake (data not shown). After screening, 4 mol % of DSPE-PEG-FA and 8 mol % of total PEG were selected to achieve an upregulated specific and active targeted delivery as well as downregulated unspecific phagocytosis.

3.7 Cellular uptake and penetration of liposomes in tumour spheroids

Tumour spheroids are three-dimensional (3D) tumour cell clusters [41], which possess similar characteristics of tumour xenografts, such as extracellular matrix, cell-cell interactions [42], spatial geometry [43] and hypoxic or necrotic regions [44]. Therefore, compare with the 2D cellular uptake experiments aforementioned, 3D tumour spheroid uptake might give a more accurate prediction of liposomes' tumour accumulation, penetration and internalisation. Plain-Lip, PEG-Lip and FA-Lip were incubated with MCF-7 and SKOV3 tumour spheroids for 24 h. Fig. 7A and Fig. 7B show the accumulation of three liposome formulations in tumour spheroids. Plain-Lip exhibited relatively high accumulation in both MCF-7 and SKOV3 tumour spheroids, while PEG-Lip showed negligible accumulation. The accumulation of FA-Lip in SKOV3 tumour spheroids was much higher than that in the MCF-7 spheroid, consistent with 2D cellular uptake experiments. A quantitative analysis of the cellular uptake of the liposomes by the tumour spheroids was conducted by dissociating the spheroids into cell suspension at the incubation time of 4 h, which was the same as the 2D cellular uptake experiments. Fig. 7C shows that 4 h incubation already showed a significant difference between the untargeted and targeted liposomes. The cellular uptake of FA-Lip by SKOV3 tumour spheroids was 90% higher than that of PEG-Lip. However no significant difference was observed for the MCF-7 tumour spheroids. Layer-by-layer scanning also showed that FA-Lip had increased accumulation in each layer of the SKOV3 tumour spheroid in comparison with the Plain-Lip and the PEG-Lip. The cellular uptake of the targeted liposome formulation FA-Lip by the 3D tumour spheroids and 2D monolayer cell culture showed consistent upregulated receptor-specific endocytosis, indicating the potential of this targeted liposome for actual applications.

To further explore the tumour penetration capability of the liposomes, the distribution of Plain-Lip, PEG-Lip and FA-Lip on SKOV3 tumour spheroids at a depth of 80 μm was extracted (bright field was removed). The distribution of fluorescence intensity along the line across the spheroid centre was recorded. Fig. 8 shows much higher fluorescence intensity peaks on the edges of the spheroid for the FA-Lip, but not for the PEG-Lip. This indicated that even though the overall cellular uptake of the targeted liposome was increased, their penetration into the tumour spheroids was limited.

Similar to 2D cell monolayer, Plain-Lip could be internalised into both the MCF-7 and SKOV3 tumour spheroids through non-specific binding while sterically stabilised PEG-Lips were not able to interact with any spheroids due to the effect of the PEG, which was in accordance with previously reported work using tumour spheroids [45]. FA-Lip possessed an overall enhanced

accumulation in the SKOV3 spheroid, however this mainly occurred at a depth of less than 60 μm. The microenvironment in tumour spheroids plays a decisive role in tumour penetration. With the formation of compact cell-cell interactions and high interstitial pressure in the tumour spheroids, it is not surprising to find limited penetration of the targeted liposome. Strategies such as using ultra-small nanoparticles [46], incorporating cell penetrating peptide (CPP) [47] or tumour penetrating peptide [48] could be used to increase tumour penetration in future studies.

Conclusion

Three liposome formulations, plain liposome, PEGylated liposome and folic acid modified liposomes (FA-Lip) were successfully synthesised using a single-step microfluidic hydrodynamic flow focusing technology. Liposomes can be precisely controlled with tunable size, narrow size distribution and varied surface modification (PEGylation and active targeting). The biological function experiments demonstrated the downregulated phagocytosis of the PEG-Lip in comparison with the Plain-Lip. And the incorporation of the targeting ligand folic acid to the liposome upregulated not only the cellular uptake using a 2D cell culture model but also the 3D tumour spheroids. The enhanced cellular uptake was demonstrated to be ligand-receptor specific endocytosis. However, although the active targeted liposome (FA-Lip) exhibited higher tumour accumulation, the penetration depth was limited to 40-60 μm. Therefore, liposomes incorporating both the active targeting and tumour penetration enhancement will be desirable to achieve better drug delivery efficiency. Because of the simplicity and versatility of this single-step microfluidic HFF technology, it holds great potential in making various kinds of liposome formulations for actual applications.

Acknowledgement

This project is supported by the Australian Research Council (ARC) Future Fellowship Project (FT140100726). Rui acknowledges PhD scholarships from the University of Queensland. This work was performed in part at the Queensland node of the Australian National Fabrication Facility, a company established under the National Collaborative Research Infrastructure Strategy to provide nano and micro-fabrication facilities for Australia's researchers. The

authors acknowledge the facilities, and the scientific and technical assistance, of the Australian Microscopy & Microanalysis Research Facility at the Centre for Microscopy and Microanalysis, The University of Queensland.

References

[1] Y. Barenholz, Doxil(R)--the first FDA-approved nano-drug: lessons learned, Journal of controlled release : official journal of the Controlled Release Society, 160 (2012) 117-134.
[2] J.C. Kraft, J.P. Freeling, Z. Wang, R.J. Ho, Emerging research and clinical development trends of liposome and lipid nanoparticle drug delivery systems, Journal of pharmaceutical sciences, 103 (2014) 29-52.
[3] G. Bozzuto, A. Molinari, Liposomes as nanomedical devices, International journal of nanomedicine, 10 (2015) 975.
[4] T.M. Allen, P.R. Cullis, Liposomal drug delivery systems: from concept to clinical applications, Advanced drug delivery reviews, 65 (2013) 36-48.
[5] D. van Swaay, A. deMello, Microfluidic methods for forming liposomes, Lab on a chip, 13 (2013) 752-767.
[6] K. Funakoshi, H. Suzuki, S. Takeuchi, Formation of giant lipid vesiclelike compartments from a planar lipid membrane by a pulsed jet flow, Journal of the American Chemical Society, 129 (2007) 12608-12609.
[7] R.T. Davies, D. Kim, J. Park, Formation of liposomes using a 3D flow focusing microfluidic device with spatially patterned wettability by corona discharge, Journal of Micromechanics and Microengineering, 22 (2012) 055003.
[8] R. Karnik, F. Gu, P. Basto, C. Cannizzaro, L. Dean, W. Kyei-Manu, R. Langer, O.C. Farokhzad, Microfluidic platform for controlled synthesis of polymeric nanoparticles, Nano letters, 8 (2008) 2906-2912.
[9] A. Jahn, W.N. Vreeland, M. Gaitan, L.E. Locascio, Controlled vesicle self-assembly in microfluidic channels with hydrodynamic focusing, Journal of the American Chemical Society, 126 (2004) 2674-2675.
[10] P.M. Valencia, P.A. Basto, L. Zhang, M. Rhee, R. Langer, O.C. Farokhzad, R. Karnik, Single-step assembly of homogenous lipid-polymeric and lipid-quantum dot nanoparticles enabled by microfluidic rapid mixing, ACS nano, 4 (2010) 1671-1679.
[11] J.M. Zook, W.N. Vreeland, Effects of temperature, acyl chain length, and flow-rate ratio on liposome formation and size in a microfluidic hydrodynamic focusing device, Soft Matter, 6 (2010) 1352-1360.
[12] A. Jahn, S.M. Stavis, J.S. Hong, W.N. Vreeland, D.L. DeVoe, M. Gaitan, Microfluidic mixing and the formation of nanoscale lipid vesicles, ACS nano, 4 (2010) 2077-2087.
[13] R.R. Hood, D.L. DeVoe, A. Andar, P.W. Swaan, D.M. Omiatek, W.N. Vreeland, Microfluidic synthesis of PEGylated liposomes, Microsystems for Measurement and Instrumentation (MAMNA), 2012, IEEE, 2012, pp. 1-4.
[14] R.R. Hood, C. Shao, D.M. Omiatek, W.N. Vreeland, D.L. DeVoe, Microfluidic synthesis of PEG- and folate-conjugated liposomes for one-step formation of targeted stealth nanocarriers, Pharmaceutical research, 30 (2013) 1597-1607.
[15] R.R. Hood, D.L. DeVoe, High-Throughput Continuous Flow Production of Nanoscale Liposomes by Microfluidic Vertical Flow Focusing, Small, 11 (2015) 5790-5799.

[16] M.B. Romanowsky, A.R. Abate, A. Rotem, C. Holtze, D.A. Weitz, High throughput production of single core double emulsions in a parallelized microfluidic device, Lab on a chip, 12 (2012) 802-807.
[17] D. Liu, A. Mori, L. Huang, Role of liposome size and RES blockade in controlling biodistribution and tumor uptake of GM1-containing liposomes, Biochimica et biophysica acta, 1104 (1992) 95-101.
[18] A. Nagayasu, T. Shimooka, Y. Kinouchi, K. Uchiyama, Y. Takeichi, H. Kiwada, Effects of fluidity and vesicle size on antitumor activity and myelosuppressive activity of liposomes loaded with daunorubicin, Biological & pharmaceutical bulletin, 17 (1994) 935-939.
[19] F. Yuan, M. Leunig, S.K. Huang, D.A. Berk, D. Papahadjopoulos, R.K. Jain, Microvascular permeability and interstitial penetration of sterically stabilized (stealth) liposomes in a human tumor xenograft, Cancer research, 54 (1994) 3352-3356.
[20] D. Liu, L. Huang, Size homogeneity of a liposome preparation is crucial for liposome biodistribution in vivo, Journal of Liposome Research, 2 (1992) 57-66.
[21] V. Torchilin, Tumor delivery of macromolecular drugs based on the EPR effect, Advanced drug delivery reviews, 63 (2011) 131-135.
[22] J. Leng, S.U. Egelhaaf, M.E. Cates, Kinetics of the micelle-to-vesicle transition: aqueous lecithin-bile salt mixtures, Biophysical journal, 85 (2003) 1624-1646.
[23] O. Garbuzenko, Y. Barenholz, A. Priev, Effect of grafted PEG on liposome size and on compressibility and packing of lipid bilayer, Chemistry and physics of lipids, 135 (2005) 117-129.
[24] Y. Xia, J. Tian, X. Chen, Effect of surface properties on liposomal siRNA delivery, Biomaterials, 79 (2016) 56-68.
[25] J.K. Kim, S.H. Choi, C.O. Kim, J.S. Park, W.S. Ahn, C.K. Kim, Enhancement of polyethylene glycol (PEG)-modified cationic liposome-mediated gene deliveries: effects on serum stability and transfection efficiency, The Journal of pharmacy and pharmacology, 55 (2003) 453-460.
[26] C. He, Y. Hu, L. Yin, C. Tang, C. Yin, Effects of particle size and surface charge on cellular uptake and biodistribution of polymeric nanoparticles, Biomaterials, 31 (2010) 3657-3666.
[27] C.R. Miller, B. Bondurant, S.D. McLean, K.A. McGovern, D.F. O'Brien, Liposome-cell interactions in vitro: effect of liposome surface charge on the binding and endocytosis of conventional and sterically stabilized liposomes, Biochemistry, 37 (1998) 12875-12883.
[28] F. Alexis, E. Pridgen, L.K. Molnar, O.C. Farokhzad, Factors affecting the clearance and biodistribution of polymeric nanoparticles, Molecular pharmaceutics, 5 (2008) 505-515.
[29] L.R. Coney, A. Tomassetti, L. Carayannopoulos, V. Frasca, B.A. Kamen, M.I. Colnaghi, V.R. Zurawski, Jr., Cloning of a tumor-associated antigen: MOv18 and MOv19 antibodies recognize a folate-binding protein, Cancer research, 51 (1991) 6125-6132.
[30] N. Parker, M.J. Turk, E. Westrick, J.D. Lewis, P.S. Low, C.P. Leamon, Folate receptor expression in carcinomas and normal tissues determined by a quantitative radioligand binding assay, Analytical biochemistry, 338 (2005) 284-293.
[31] J. Pan, S.S. Feng, Targeting and imaging cancer cells by folate-decorated, quantum dots (QDs)-loaded nanoparticles of biodegradable polymers, Biomaterials, 30 (2009) 1176-1183.
[32] H. Chen, R. Ahn, J. Van den Bossche, D.H. Thompson, T.V. O'Halloran, Folate-mediated intracellular drug delivery increases the anticancer efficacy of nanoparticulate formulation of arsenic trioxide, Molecular cancer therapeutics, 8 (2009) 1955-1963.
[33] S.D. Conner, S.L. Schmid, Regulated portals of entry into the cell, Nature, 422 (2003) 37-44.
[34] D. Zhang, H. Xu, M.N. Hu, Y.H. Deng, ["PEG dilemma" for liposomes and its solving approaches], Yao xue xue bao = Acta pharmaceutica Sinica, 50 (2015) 252-260.
[35] H. Du, P. Chandaroy, S.W. Hui, Grafted poly-(ethylene glycol) on lipid surfaces inhibits protein adsorption and cell adhesion, Biochimica et biophysica acta, 1326 (1997) 236-248.
[36] K. Maruyama, O. Ishida, T. Takizawa, K. Moribe, Possibility of active targeting to tumor tissues with liposomes, Advanced drug delivery reviews, 40 (1999) 89-102.
[37] J. Sudimack, R.J. Lee, Targeted drug delivery via the folate receptor, Advanced drug delivery reviews, 41 (2000) 147-162.

[38] R.J. Lee, P.S. Low, Delivery of liposomes into cultured KB cells via folate receptor-mediated endocytosis, Journal of Biological Chemistry, 269 (1994) 3198-3204.
[39] A. Gabizon, A.T. Horowitz, D. Goren, D. Tzemach, F. Mandelbaum-Shavit, M.M. Qazen, S. Zalipsky, Targeting folate receptor with folate linked to extremities of poly(ethylene glycol)-grafted liposomes: in vitro studies, Bioconjugate chemistry, 10 (1999) 289-298.
[40] J. Reddy, C. Abburi, H. Hofland, S. Howard, I. Vlahov, P. Wils, C. Leamon, Folate-targeted, cationic liposome-mediated gene transfer into disseminated peritoneal tumors, Gene therapy, 9 (2002).
[41] R.M. Sutherland, Cell and environment interactions in tumor microregions: the multicell spheroid model, Science, 240 (1988) 177-184.
[42] T. Nederman, B. Norling, B. Glimelius, J. Carlsson, U. Brunk, Demonstration of an extracellular matrix in multicellular tumor spheroids, Cancer research, 44 (1984) 3090-3097.
[43] L. Davies Cde, D.A. Berk, A. Pluen, R.K. Jain, Comparison of IgG diffusion and extracellular matrix composition in rhabdomyosarcomas grown in mice versus in vitro as spheroids reveals the role of host stromal cells, British journal of cancer, 86 (2002) 1639-1644.
[44] A. Gorlach, H. Acker, pO2- and pH-gradients in multicellular spheroids and their relationship to cellular metabolism and radiation sensitivity of malignant human tumor cells, Biochimica et biophysica acta, 1227 (1994) 105-112.
[45] L. Mei, L. Fu, K. Shi, Q. Zhang, Y. Liu, J. Tang, H. Gao, Z. Zhang, Q. He, Increased tumor targeted delivery using a multistage liposome system functionalized with RGD, TAT and cleavable PEG, International journal of pharmaceutics, 468 (2014) 26-38.
[46] K. Huang, H. Ma, J. Liu, S. Huo, A. Kumar, T. Wei, X. Zhang, S. Jin, Y. Gan, P.C. Wang, S. He, X. Zhang, X.J. Liang, Size-dependent localization and penetration of ultrasmall gold nanoparticles in cancer cells, multicellular spheroids, and tumors in vivo, ACS nano, 6 (2012) 4483-4493.
[47] W. Gao, B. Xiang, T.-T. Meng, F. Liu, X.-R. Qi, Chemotherapeutic drug delivery to cancer cells using a combination of folate targeting and tumor microenvironment-sensitive polypeptides, Biomaterials, 34 (2013) 4137-4149.
[48] T. Teesalu, K.N. Sugahara, E. Ruoslahti, Tumor-penetrating peptides, Frontiers in oncology, 3 (2013) 216.

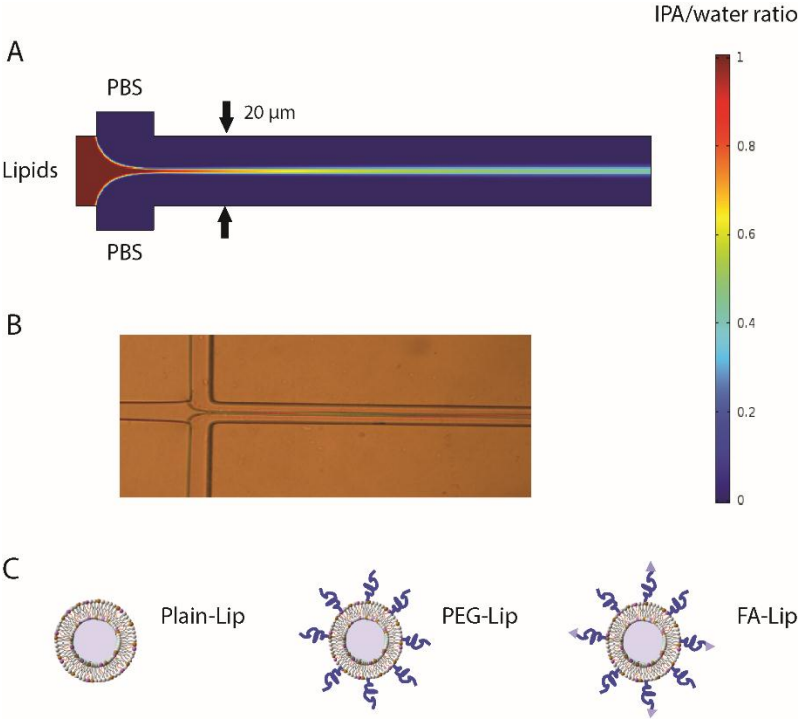

Fig. 1 Numerical simulation (A) and optical micrograph (B) of liposome synthesis in the hydrodynamic flow focusing device at a flow rate ratio of 12:1. The width of the microchannels is 20 µm, the height is 60 µm and the total length of the central channel is 1 cm. (C) Schematic illustrations of Plain-Lip, PEG-Lip and FA-Lip.

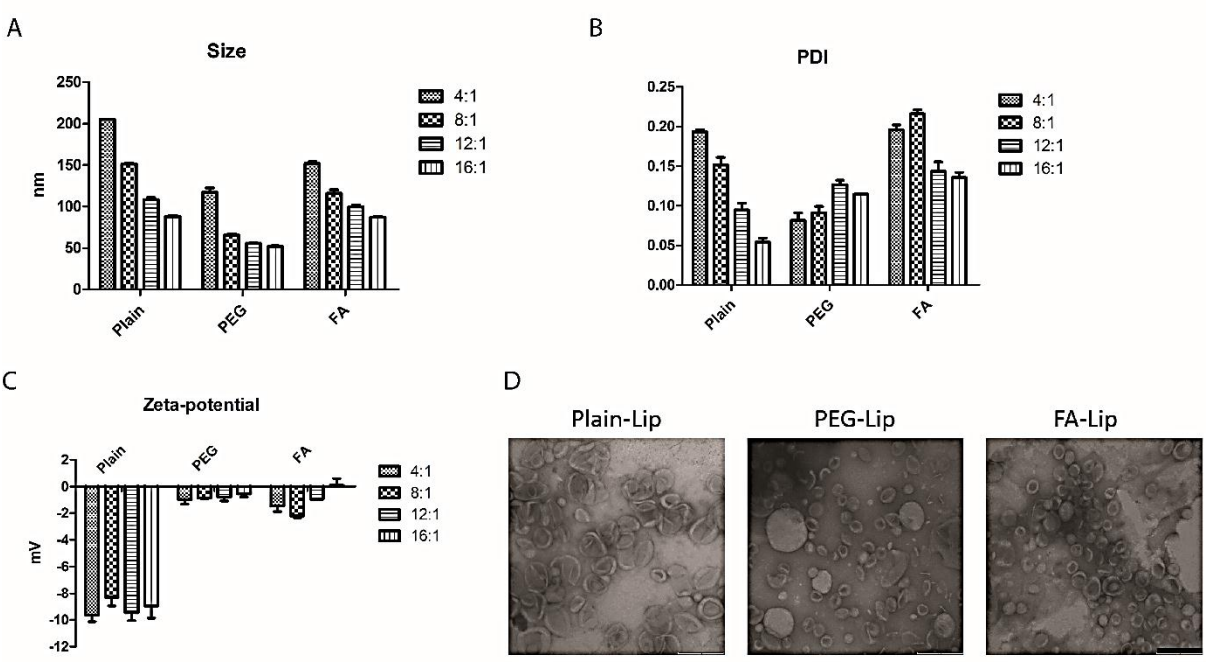

Fig. 2 Characterisation of Plain-Lip, PEG-Lip and FA-Lip at different FRRs. (A) size, (B) PDI and (C) zeta-potential. (Mean ± SD, n = 3; n represents the number

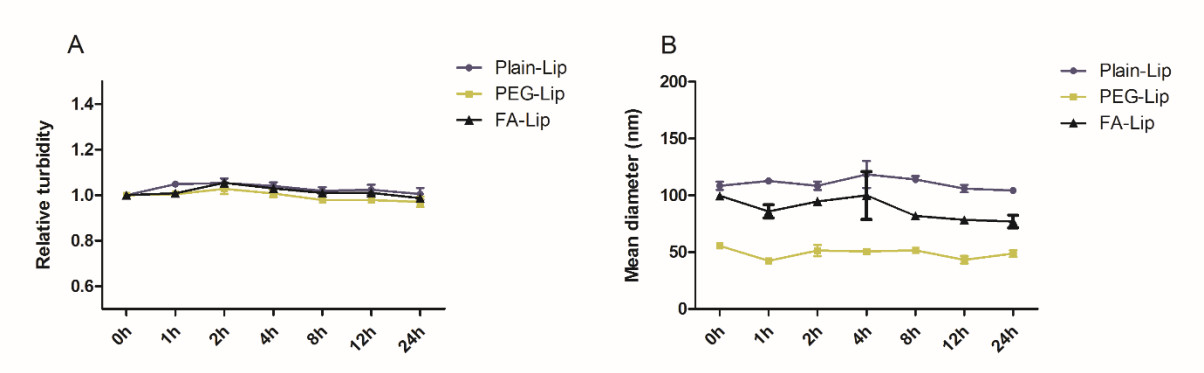

Fig. 3 Serum stability of the three liposome formulations. (A) Relative turbidity and (B) mean diameter of Plain-Lip, PEG-Lip and FA-Lip in 50% FBS. (Mean ± SD, for relative turbidity, n = 5 and for mean diameter, n = 3; n represents the number of independent samples)

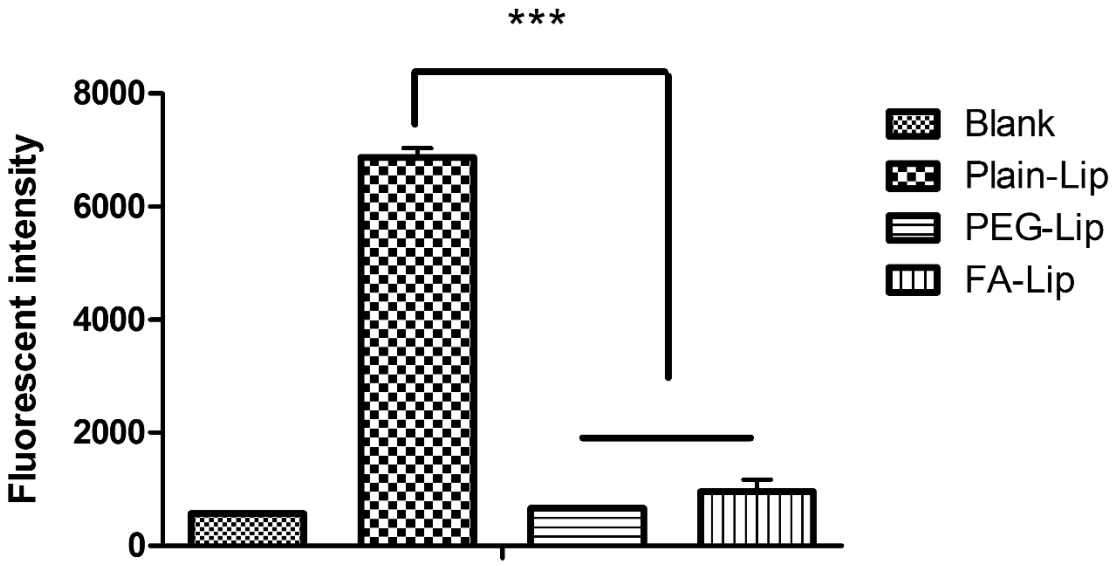

Fig. 4 RAW 264.7 uptake of DiI-labelled liposomes, *** represents statistically significant difference ($p < 0.001$). (Mean ± SD, n = 3; n represents the number of independent samples)

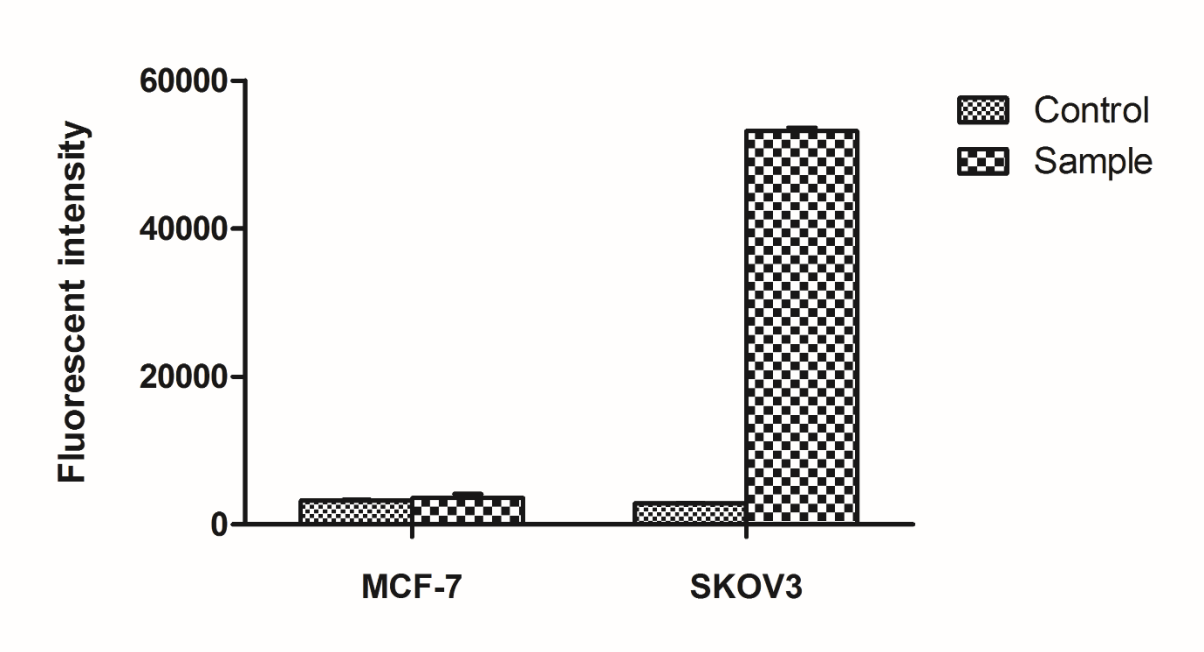

Fig .5 Folate receptor expression determined by flow cytometry. Cells incubated with a secondary antibody were regarded as the control group and cells incubated with both the primary and secondary antibodies were regarded as the sample group. (Mean ± SD, n = 3; n represents the number of independent samples)

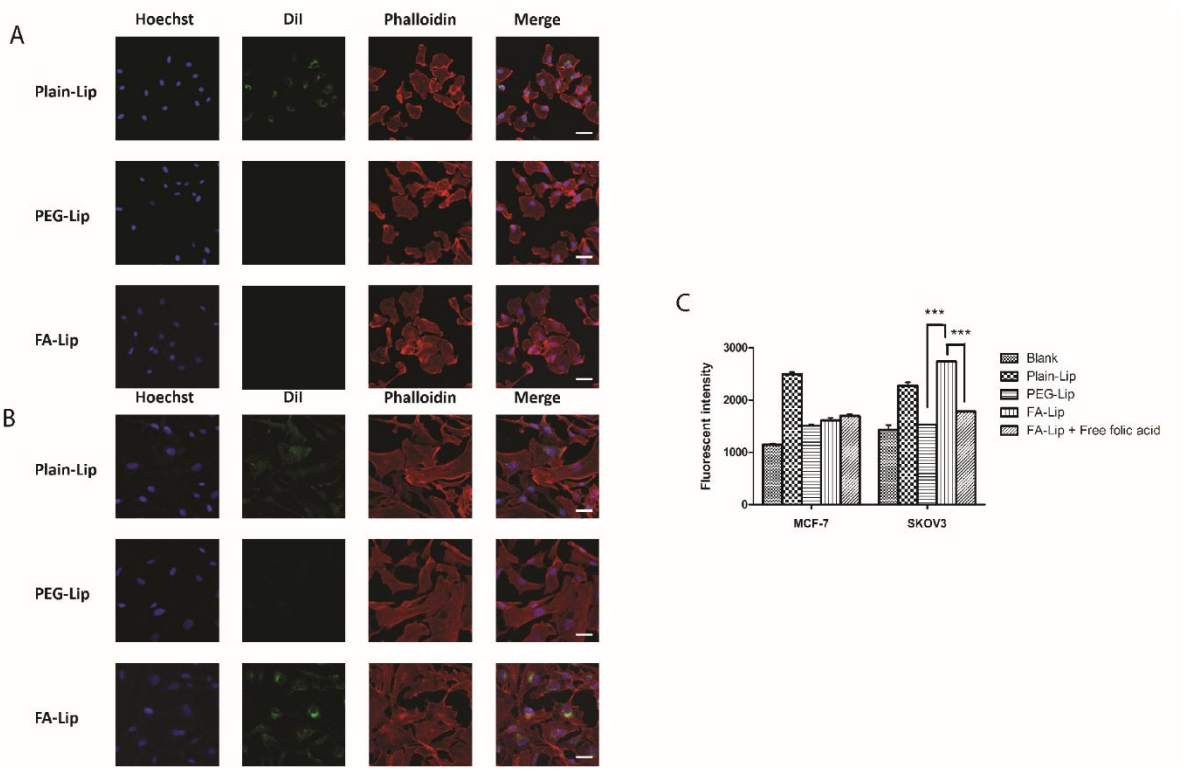

Fig. 6 Cellular uptake of DiI labelled liposomes determined by CLSM on MCF-7 (A) and SKOV3 (B) cells. (C) Flow cytometry determination. Scale bars represent 20 μm. *** represents statistically significant difference ($p < 0.001$). (Mean ± SD, n = 3; n represents the number of independent samples)

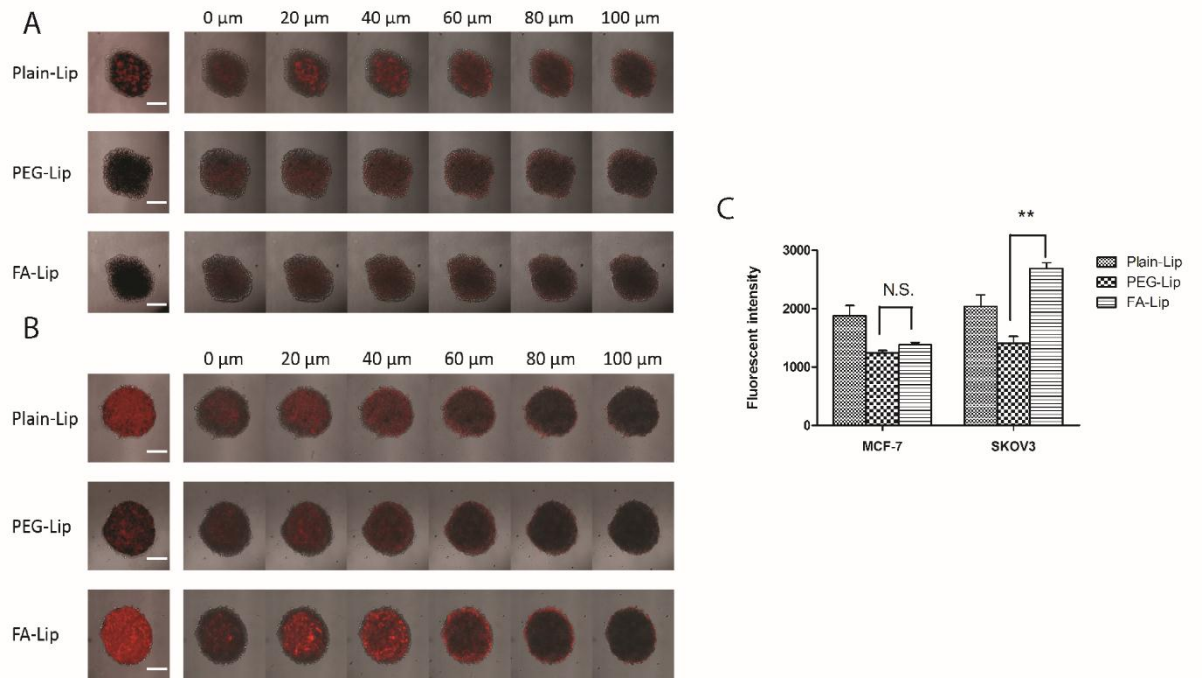

Fig. 7 CLSM observations of overall and layer-by-layer images of DiI labelled liposomes in (A) MCF-7 tumour spheroids and (B) SKOV3 tumour spheroids. Scale bars represent 200 μm. (C) Quantitative analysis of cellular internalisation of DiI labelled liposomes in 3D tumour spheroids. ** represents statistically significant difference ($p < 0.01$). N.S. represents no statistical significant difference (Mean ± SD, n = 3; n represents the number of tumour spheroids).

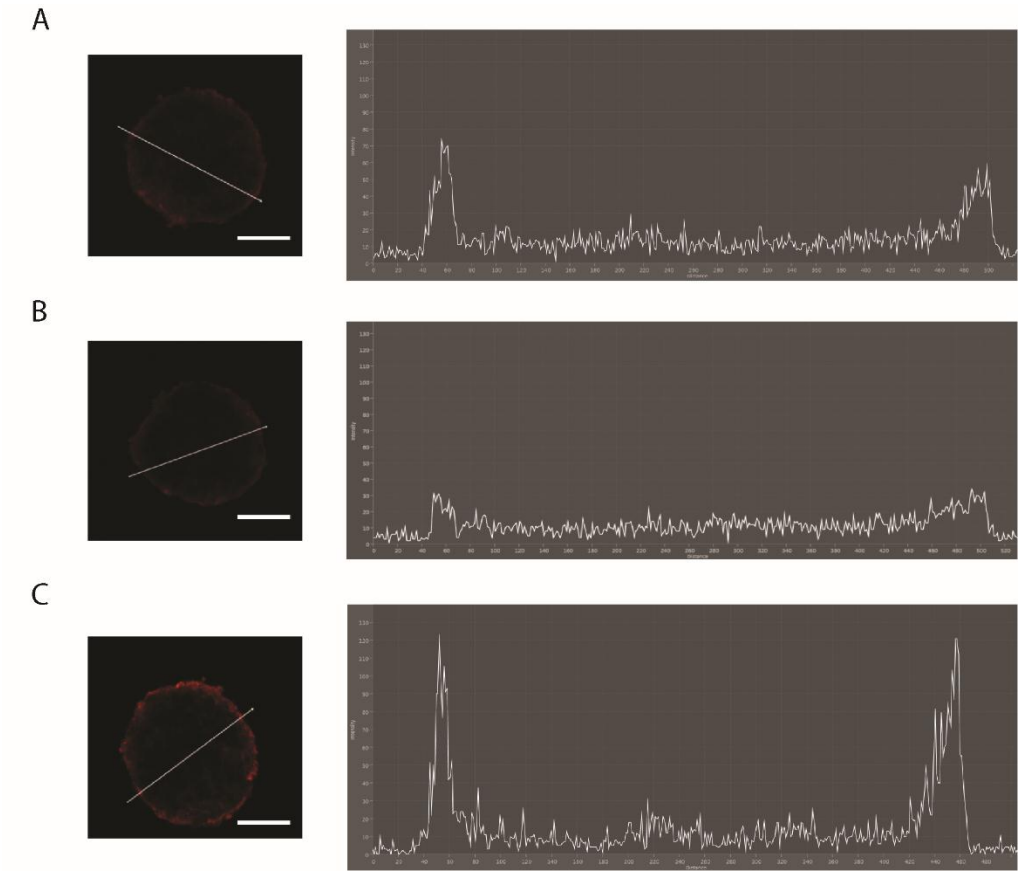

Fig. 8 DiI fluorescence intensity distribution along the line across the centre of the SKOV3 tumour spheroids at the depth of 80 µm of (A) Plain-Lip, (B) PEG-Lip and (C) FA-Lip. Bright fields are excluded. Scale bars represent 200 µm.